

Estimating the Life Time Span of Aswan High Dam Reservoir Using Numerical Simulation of Nubia Lake

Abdelazim M. Negm, Tarek Abdel-Aziz, Mohamed Nassar,
and Ismail Fathy

Abstract It is expected that the Grand Ethiopian Renaissance Dam (GERD) will be completed and put into operation within few years. The pattern of sedimentation will be affected as well as the amount of sediment accumulation in the Aswan High Dam Reservoir (AHDR). Also, the life time span of AHDR will be greatly affected. In this chapter, a two-dimensional numerical model CCHE2D is applied to study the scouring and silting processes in AHDR from km 500 to km 350 upstream Aswan High Dam (AHD). The sediment transport is simulated in terms of the depth-averaged sediment concentration. The different cross sections along Nubia Lake (Sudanese part of the reservoir) are predicted for the year 2010 and the year 2020. Statistical indicators showed that the model results are accurate enough to be used to predict the morphological changes and the life time span of AHDR. The results show that the life time span of dead zone (LTSDZ) is 254 years, while life time span of life zone (LTSLZ) is 964 years.

Keywords Aswan High Dam, CCHE2D, Life time span, Reservoir, Sediment transport

Contents

1	Introduction	36
2	Study Area and Data Collection	38
3	Simulation Model (CCHE2D)	40
4	Boundary and Initial Conditions	41

A.M. Negm (✉), M. Nassar, and I. Fathy
Water and Water Structures Engineering Department, Faculty of Engineering, Zagazig
University, Zagazig 44519, Egypt
e-mail: amnegg85@yahoo.com; amnegg@zu.edu.eg

T. Abdel-Aziz
Nile Research Institute, NWRC, MWRI, Ashmoun, Egypt
e-mail: Aziztm@hotmail.com

5	Model Calibration	42
6	Model Verification	43
7	Predication of Life Time Span of AHDR	46
7.1	Using the Traditional Method	46
7.2	Using the CCHE2D Simulation Model	48
8	Conclusions and Recommendations	48
	Appendix: Initial and Boundary Conditions Data of Section 4	51
	References	54

1 Introduction

Reservoirs contribute by 20% of the international generation of electricity, World Commission on Dams [1]. As a result, the increasing of the lifetime of reservoirs is an urgent need. Processes of sedimentation control the lifetime of reservoirs, Morris and Fan [2]. The sedimentation processes decreased the lifetime of many reservoirs in the USA by 50:100 years, Hargrove et al. [3]. The capacity of the total reservoirs in China was decreased by 66%, Wang and Hu [4]. Moreover, the capacity of California statewide reservoir decreased by 4.5%, Minear and Kondolf [5]. Wang [6] indicated that the dams' lifetime is limited. It may reach to 100 years, Morris and Fan [2]. It was reported that the processes of sedimentation reduced the average storage capacity by 35% for 14 reservoirs in Puerto Rico, Soler-López [7] and Angulo et al. [8]. Issa et al. [9] concluded that the yearly decrease of dead and life storage capacities of Iraqi Mosul reservoir using a bathymetric survey and an analytical technique is 0.786% and 0.276%, respectively. Dalu et al. [10] detected the life of siltation for Zimbabwean Malilangwe reservoir as 100 years using the Wallingford method. Wissner et al. [11] detected the reduction of the reservoirs' capacity by 5% for international reservoirs' data sets from 1901 to 2010.

On the other hand, the parameters of sediments through AHDR were defined by Makary [12]. The volume of the deposition for AHDR through the period from 1964 to 1985 was estimated by El-Moattassem and Makary [13] to be about 1,650 Mm³. The lifetime of AHD was expected to be 362 years, Shalash [14]. The dead zone of the reservoir was expected to be 310 years, Dahab [15]. Further investigations on the bed profile were made by Abdel-Aziz [16, 17]. In 1991, Abdel-Aziz simulated the bed profile of Aswan High Dam Reservoir in the longitudinal direction by 1D model. The bed profile of AHDR in both longitudinal and transverse directions was predicted, Abdel-Aziz [17]. The regions of the sedimentations in AHDR were defined using GIS, El-Sersawy [18]. The base map of AHDR was presented for the year 2006 by Amary [19]. Recently, Moussa [20] predicted bathymetric change along a 150 km of AHDR from 2009 to 2014 using CCHE2D. It was indicated that the maximum depositions and erosions were 3.71 m and 3.8 m, respectively.

Moreover, Hekal and Abdel-Aziz [21] recommended the use of the average transverse velocity to predict the patterns of the deposition through AHDR. Ziada

[22] indicated the important effect of the flow decrease on the analysis of the sedimentation processes. Hassan [23] found that Sudanese Merowe Dam and Ethiopian Tekeze Dam caused negative side effects on the inflow discharge to HADR. Elsayhaby et al. [24] generated a 3D layer of the condensed deposition zone in Lake Nasser by remote sensing and GIS techniques. Elsayeed et al. [25] predicted the sedimentation of AHDR from 2010 to 2025 using Delft3D. It was indicated that the maximum depositions and erosions were 15.6 m and 1.75 m, respectively.

On the other hand, many studies were interested in computing the life time span of AHDR as indicated by Table 1.

In this chapter CCHE2D is applied to estimate the life time span of AHDR by investigating the sedimentation processes through the 150 km of Sudanese part (Nubia Lake). Also, the model is applied to detect lateral bed profiles for the year 2010 and the year 2020. The predicted values using CCHE2D are compared to those computed using the traditional method.

Table 1 Estimated useful life (or sediment accumulated/sediment rate) based on previous investigators since 1964 till 2016, Fathy [26] and Moussa [20]

Author	Year	Conclusion
French engineering	1891	Annual rate of sediment deposition of 1 mm on the temporarily flooded lands in Egypt
Russian engineering	Prior 1964	Dead zone 500 years
Hurst	1965	30% sand, 40% silt, and 30% clay
Ho-Khteef German Co.	1970	Dead zone 750 years
American Building Authority	1970	Dead zone 1,000 years
Abu-EL Ata	1978	Dead zone 440 years
Shalash	1980	Sedimentation 1,570 million tons during 15-year period between 1964 and 1979; dead zone 362 years
Makary	1982	Dead zone 408 years and total life 1,580 years
Dahab	1982	Dead zone 310 years
El-Moattassem	1988	Sediment 1,650 million tons during 21-year period between 1964 and 1985
El-Manadely	1991	Sedimentation 2,650 million tons during 24 years
Abdel-Aziz	1997	Dead zone 311 year and life zone 1,202 years
NRI	2003	Estimated that more than 5.2 billion tons (1964–2003)
NRI	2008	Estimated that more than 6.285 billion tons (1964–2008)
Negm et al.	2010	The accumulated sediment since 1964 till 2010 is 4,936 billion M ³
Moussa	2012	The CCHE2D prediction indicated that the bed level changed with depositions ranging from 3.71 to 0.3 m and erosion ranging from 3.8 to 0.09 m. Further analysis indicated that trend of channel bed change differs only for 25% of cross sections while it remains the same for the rest of sections
Present	2016	The predicted life time span of AHDR is 964 on the year 2020

2 Study Area and Data Collection

The study is located in AHDR from km 500 to km 350 upstream High Aswan Dam with a total length of 150 km in Sudan where the delta is formed (see Fig. 1). This part includes 15 cross sections as indicated in Fig. 1. The section code, the distance of the section from upstream the AHD, the width of the section, and the length represented by the section are presented in Table 2. The bed level, velocities, discharges, and suspended concentration were collected from the Nile Research Institute (NRI), National Water Research Center (NWR), and Ministry of Irrigation and Water Resources (MIWR). The collected data were for the sections presented in Table 1. The longitudinal profile based on the lowest bed elevations of the reservoir from year 1964 to year 2007 was plotted as indicated by Fig. 2 [27]. It was observed that the thickness of the deposition layer raised by about 60 m within the last 43 years at the entrance of the reservoir.

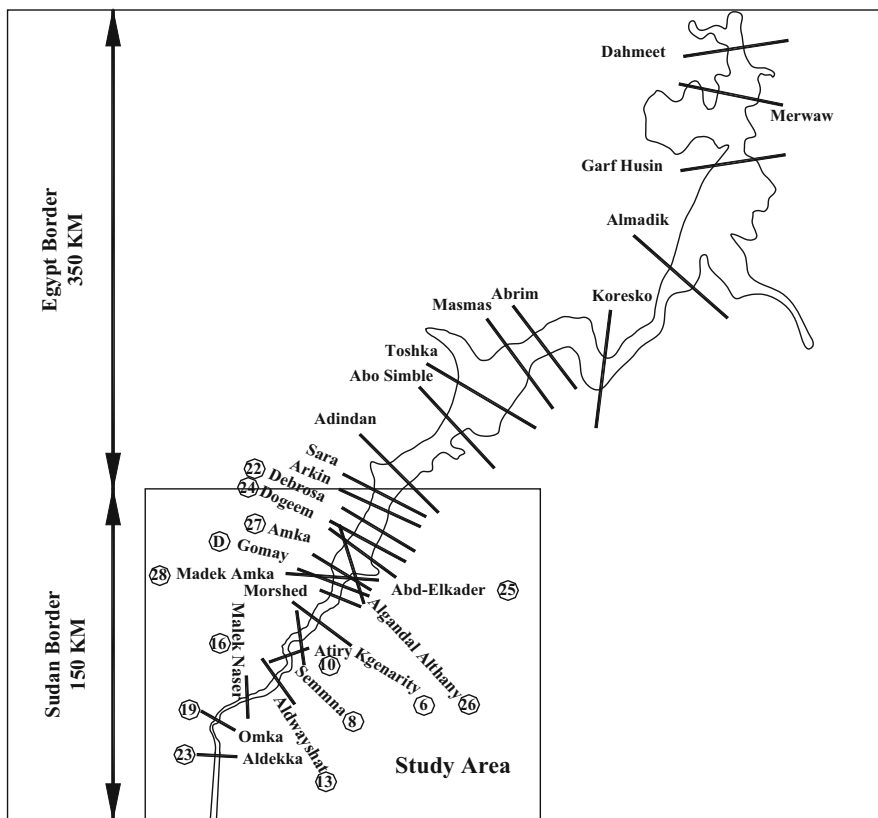


Fig. 1 A sketch for the studied area, Negm et al. [27]

Table 2 Representing length and width of each cross section, Negm et al. [27]

Section code	Name	Distance US AHD (km)	Width of cross sec (m)	Representing length (km)
23	Daka	487.50	480.0	17.00
19	Okma	466.00	610.0	19.50
16	Malik EL Nasser	448.00	1,045.0	17.50
13	EL Dowashate	431.00	1,228.50	16.25
10	Atheri	415.50	1,067.20	13.75
8	Semna	403.50	975.70	15.75
6	Kajnarity	394.00	1,281.10	12.50
3	EL Mourshed	378.50	1,278.60	11.00
D	Gami	372.00	1,605.0	5.25
28	Madik Amka	368.00	2,502.0	4.00
27	Amka	364.00	4,588.70	8.00
26	Second cataract	357.00	5,183.30	8.50
25	Abel kader	352.00	12,125.60	5.00
24	Doghim	347.00	5,559.70	7.25
22	Debrosa	337.50	9,900.0	9.00

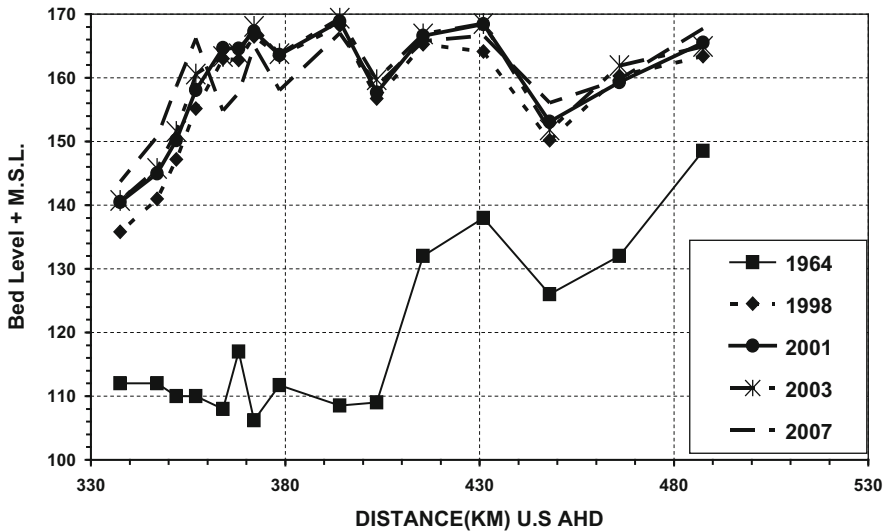


Fig. 2 Bed profile according to lowest point, Negm et al. [27]

3 Simulation Model (CCHE2D)

The CCHE2D hydrodynamic model was used to simulate the flow field. The simulation is based on the solution Navier-Stokes equations for turbulent flow. The governing equations include the momentum equations in x and y directions, the continuity equation, and sediment transport equation, Zhang [28]. The CCHE2D model is an integrated package for simulation and analysis of free surface flows, sediment transport, and morphological processes. It also includes a mesh generator (CCHE2D Mesh Generator) and a Graphical Users Interface (CCHE2D-GUI), Zhang [28]. The first module concerned with discretization of the studied area, while the second one can be considered as a visual interface. The calculation procedure of CCHE2D model can be summarized as a flowchart (see Fig. 3). The governing equations of CCHE2D used for simulating the flow field and sediment transport are continuity equation, the momentum equations in x and y directions, and sediment transport equation as presented in Eqs. (1), (2), and (3), respectively:

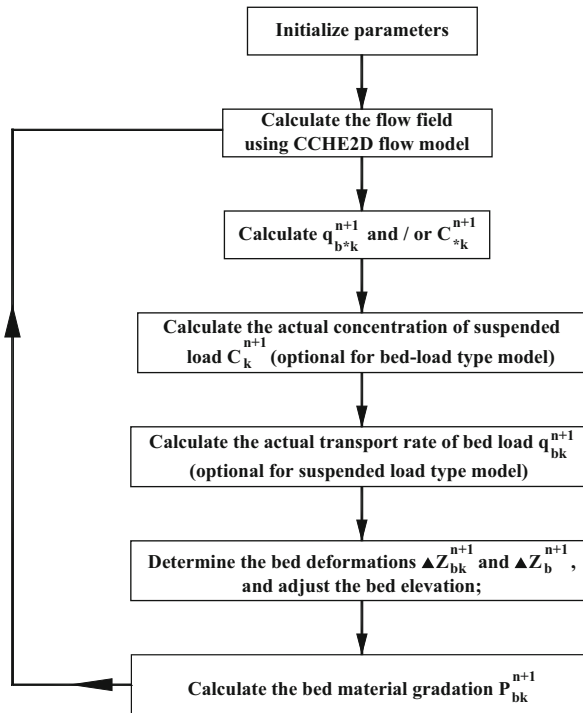


Fig. 3 Numerical model flow chart, Negm et al. [27]

Continuity equation:

$$\frac{\partial z}{\partial t} + \frac{\partial(hu)}{\partial x} + \frac{\partial(hv)}{\partial y} = 0 \quad (1)$$

Momentum equations:

$$\frac{\partial u}{\partial t} + u \frac{\partial u}{\partial x} + v \frac{\partial u}{\partial y} = -g \frac{\partial z}{\partial x} + \frac{1}{h} \left[\frac{\partial(h\tau_{xx})}{\partial x} + \frac{\partial(h\tau_{xy})}{\partial y} \right] - \frac{\tau_{bx}}{\rho h} + f_{cor}v \quad (2)$$

$$\frac{\partial v}{\partial t} + u \frac{\partial v}{\partial x} + v \frac{\partial v}{\partial y} = -g \frac{\partial z}{\partial y} + \frac{1}{h} \left[\frac{\partial(h\tau_{yx})}{\partial x} + \frac{\partial(h\tau_{yy})}{\partial y} \right] - \frac{\tau_{by}}{\rho h} + f_{cor}u \quad (3)$$

Sediment transport equation:

$$\frac{\partial c_k}{\partial t} + U \frac{\partial c_k}{\partial x} + v \frac{\partial c_k}{\partial y} = \varepsilon_s \left(\frac{\partial^2 c_k}{\partial x^2} + \frac{\partial^2 c_k}{\partial y^2} \right) + \frac{\alpha \omega_{sk}}{h} (C_{*k} - C_k) + S_c \quad (4)$$

where u is the depth-integrated velocity components in the x direction; v is the depth-integrated velocity components in the y directions; z is the water surface elevation; g is the gravitational acceleration; ρ is water density; h is the local water depth; f_{cor} is the Coriolis parameter; τ_{xx} , τ_{xy} , τ_{yx} , and τ_{yy} are the depth-integrated Reynolds stresses; τ_{bx} and τ_{by} are shear stresses on the bed surface; C_n is the concentration of n -th size class of sediment; S_c is the source term including the derivatives of ε_s and h ; z direction being assigned as the vertical direction along the gravity; ω_{sk} is the settling velocity of the n -th size class of sediment; ε_s is the eddy diffusivity of sediment, $\varepsilon_s = \nu_s/\sigma_s$; V_t is the eddy viscosity of flow; σ_s is the turbulent Prandtl-Schmidt number (between 0.50 and 1.0); S_c is the source term including the derivatives of ε_s and h ; C_k is the depth-averaged concentration; and C_{*k} is the transport capacity of total load.

4 Boundary and Initial Conditions

In the solutions of any partial differential equations, it is necessary to specify the initial state of functional domain and the conditions at its boundaries. For the study area, the initial conditions that are used during the simulation process are the cross sections of Lake Nasser (Sudanese sections) and its water levels that are surveyed at year 2003. Table 5 (see the Appendix) shows the surveyed data of section 23 (upstream section), and Table 6 (see the Appendix) shows the measured water level for the cross sections of the study area.

At the inlet boundary, the incoming discharges and sediment distribution may be considered if it is known, or it may be taken as uniform and equal to certain value.

Both two options are available in the model. For sediment transport under unsteady conditions, the time series of inflow sediment discharge is needed. In case of nonuniform sediment transport, the size distribution and of the inlet sediment is also needed. For the study area, the available incoming discharges, bed load, and suspended load are used as upstream boundary condition as shown in Tables 7, 8, and 9 (see the Appendix). Table 7 presents the measured water levels and discharge inside AHDR during the period of 1968–2007 so the data that are measured at years 2003–2007 are used for calibration and verification process, and for the predication process, the average discharge is used during verification process. Tables 8 and 9 present the sieve analysis results for the collected bed load and suspended load samples from the studied cross sections, respectively. For the outflow boundary, the corresponding water level of incoming discharge (rating curve) used during the study is shown in Table 7.

5 Model Calibration

The studied area has been schematized using a rectangular uniform mesh in the longitudinal direction with grid size ($x = 250\text{--}150\text{ m}$), while in the lateral direction, the grid size was ($y = 120\text{--}50\text{ m}$). It was very important to satisfy the hydrodynamic model calibration before using its velocity computations for prediction of sediment concentration. Therefore, the model was calibrated and verified using the velocity distribution and bed levels along the 15 sections of the studied area. The calibration procedure has been conducted by achieving, at first, the hydrodynamic simulation using the hydrodynamic model. The hydrodynamic simulation is accepted when the velocity distribution along the studied reach was almost the same as that measured one in the field. To achieve this step, the bed topography may be adopted within $\pm 0.10\text{ m}$ for a satisfactory simulation. Once the considered reach is well simulated, the suspended sediment concentrations, resulted from the sediment model, are in comparison to that measured in the field, which is called as verification stage. Moreover, the scour and silting zones may be detected and defined along the studied reach.

Plotting the results of all cross sections indicated that there is an acceptable agreement between the hydrodynamic model results and the field measurements. Typical plots for both measured and modeled depth-averaged flow velocity profiles and the corresponding waterway cross sections 13 and 16 are shown in Figs. 4 and 5, respectively. The statistical measures presented in Table 3 are evaluated using Microsoft Excel 2007. Figure 6a showed a comparison between the measured depth-averaged velocities and the predicted ones. A good agreement is observed. The residual values are plotted versus the predicted depth-averaged velocity as shown in Fig. 6b. The residuals show a random distribution around the line of zero.

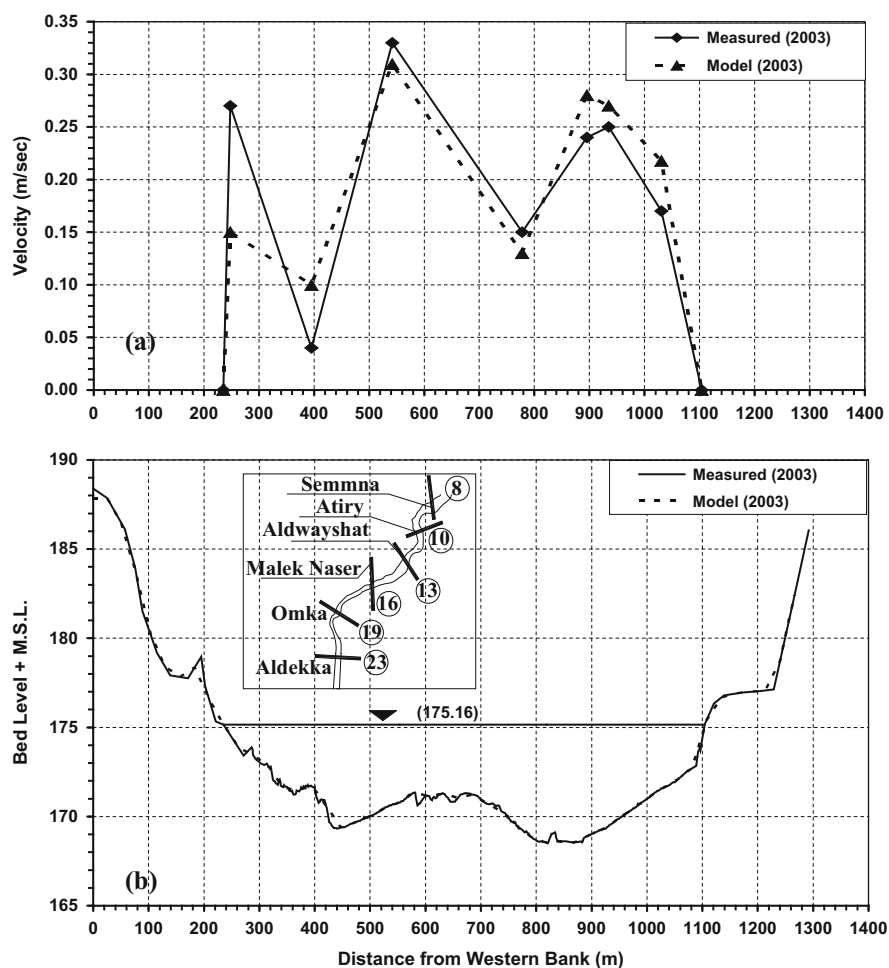


Fig. 4 (a) Measured velocities versus the computed ones using CCHE2D and (b) the measured cross section bathymetry for C.S. No. (13)

6 Model Verification

The prediction of the bed levels and the scour and silting zones are simulated using CCHE2D model. The input data includes topographic map of the studied reach, passing discharge, and the depth-averaged flow velocity field within the considered reach. The bed levels at the year 2007 are computed and compared to the field measurements at all sections. Results for two typical cross sections No.13 and No.16 are presented in Figs. 7 and 8, respectively. It can be noticed that there is an acceptable agreement between the numerical model outputs and the measurement data at the different cross sections.

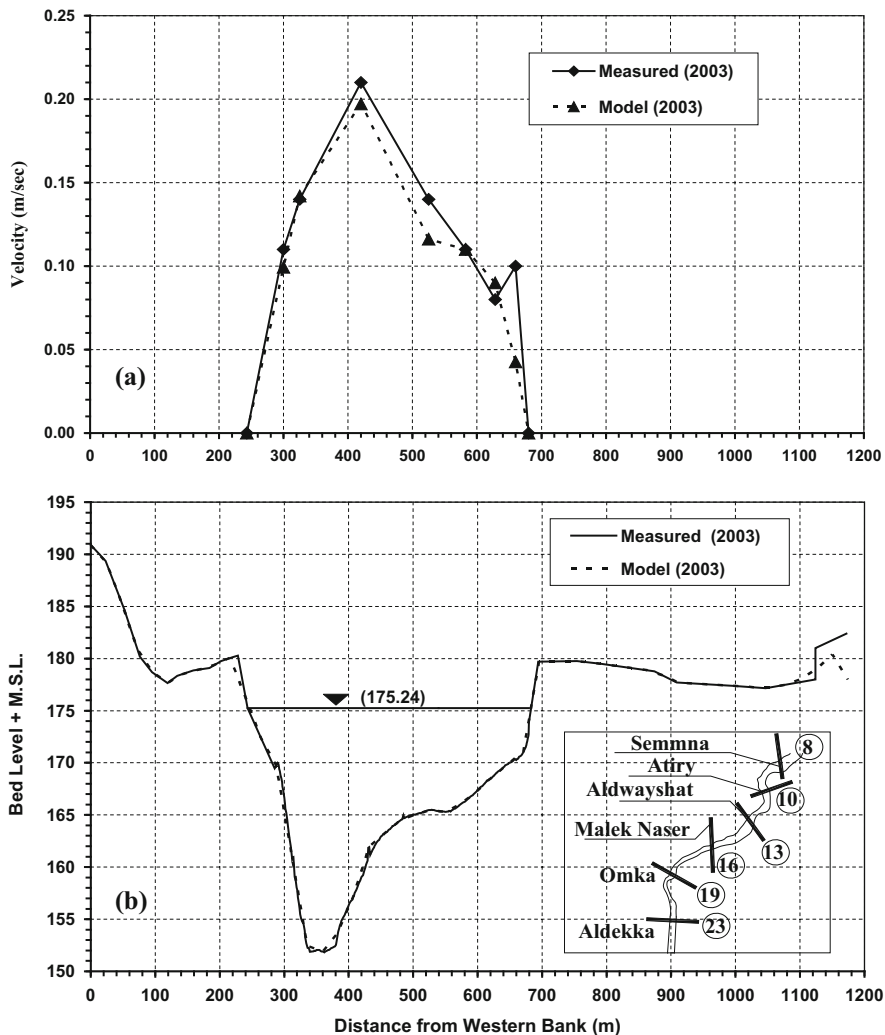


Fig. 5 (a) Measured velocities versus the computed ones using CCHE2D and (b) the measured cross section bathymetry for C.S. No. (16)

On the other hand, Fig. 9a presented a comparison between the measured bed levels and the predicted ones. An acceptable agreement is observed. The residual values are plotted versus the predicted bed levels as shown in Fig. 9b. The residuals have a random distribution around the line of zero. The statistical measures are listed in Table 2. The accuracy was more than 80%, comparing the model results and the field measurements at these sections.

Table 3 Statistical parameters for model comparison

Concept	Name	Formula	Model calibration (%)	Model verification (%)
Root m. square error	RMSE	$\sqrt{\sum_i^j (Mes - Pre)^2 / N}$	4.47	2.00
Deter. coefficient	R2	$\sum_i^j (Pre - avg.Mes)^2 / \sum_i^j (Mes - avg.Mes)^2$	75.22	85.00

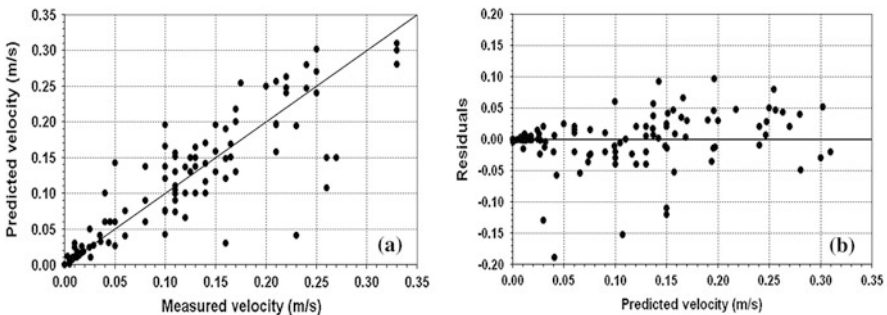


Fig. 6 (a) Predicted velocities in m/s versus measured ones in m/s and (b) variations of residuals (m/s) versus predicted values for both cross sections (13) and (16)

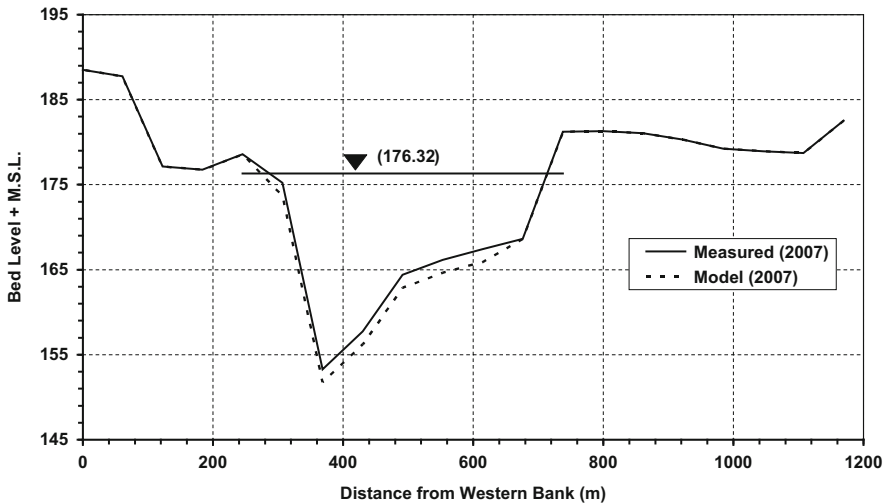


Fig. 7 Comparison between model results and the field measurements at C.S. No. 16

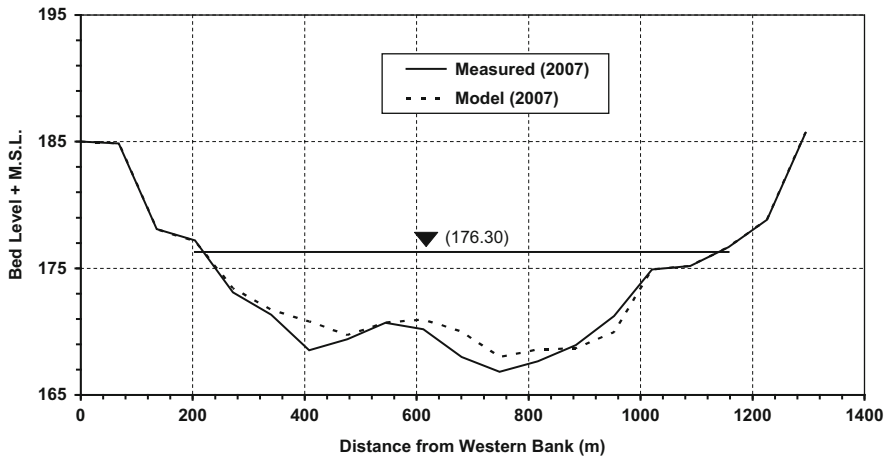


Fig. 8 Comparison between model results and the field measurements at C.S. No. 13

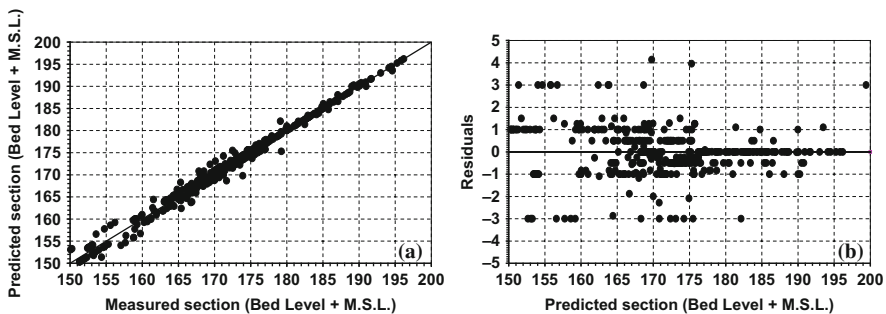


Fig. 9 (a) Predicted bathymetry in m versus measured ones in m and (b) variations of residuals (m) versus the predicted values for cross sections No. 13 and No. 16

7 Predication of Life Time Span of AHDR

The calibrated and verified CCHE2D model is applied to Nubia Lake to estimate the life time span of dead zone and life zone of the lake. In addition, the traditional method (i.e., cross-sectional method) is used to determine the life time span of the reservoir. Finally, both methods are compared.

7.1 Using the Traditional Method

Traditional method or the cross-sectional method is used to calculate the life time span of AHDR in a wide range before the year 1985 as reported in Abdel-Aziz

[16]. The procedure of the traditional method to calculate the life time span of the reservoir can be summarized as follows:

- Calculating the cross-sectional area of all sections for the year 1964 and year 2007
- Calculating deposited volume for all cross sections as indicated by Table 3
- Calculating the accumulated deposited volume in the reservoir
- Calculating the average life time span of the dead zone by dividing the designed dead storage volume of the reservoir (31.6 billion m^3) on the accumulated computed volume

The traditional method used cross sections' data for both years 1964 and 2007 to calculate the deposited area for all the 15 sections. A typical example is presented in Fig. 10 for section 19. Depending on the previous procedure and cross sections of the year 1964 and the year 2007, the accumulated deposited volume (AcDV) in Sudanese part is calculated. It equals 4,744.89 Mm^3 (see Table 3). The accumulated deposited volume in Egypt's border equals 20% of total volume deposited in Lake Nasser, Negm et al. [27]. Hence, the total accumulated volume (TAV) in the reservoir equals 5,693.9 Mm^3 . The annual deposited volume in the reservoir ($\text{ADV} = \text{AcDV}/\text{time (years)} = 132.42 \text{ Mm}^3/\text{year}$). Finally, the life time span of dead zone ($\text{LTSDZ} = (\text{DDSV}/\text{ADV}) = 239 \text{ years}$). Actually, the designed life storage volume of the reservoir ($\text{DLSV} = 90.70 \text{ billion m}^3$). Depending on the same procedure, life time span of life zone ($\text{LTSLZ} = \text{LTSDZ} + (\text{DLSV}/\text{ADV}) = 924 \text{ years}$).

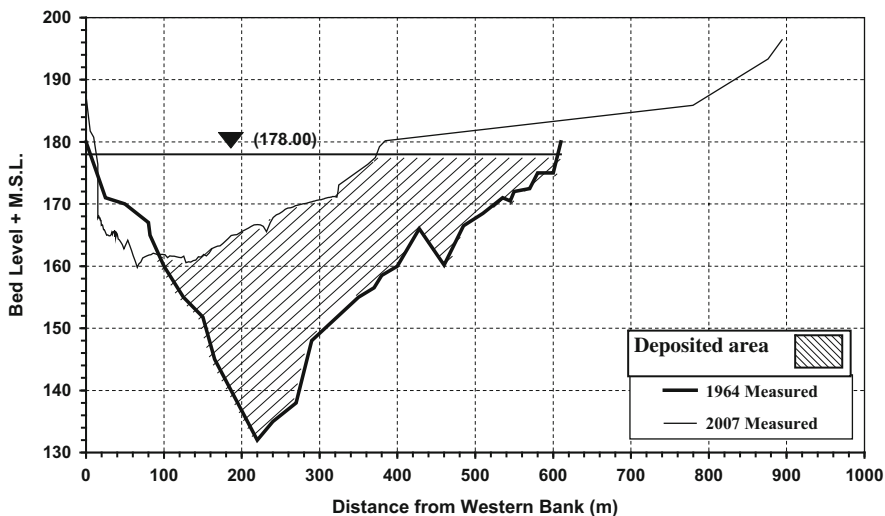


Fig. 10 Sediment accumulation at cross section 19 km 466 upstream AHD using the traditional method for the year 2007

7.2 Using the CCHE2D Simulation Model

The calibrated and verified CCHE2D model is applied to predict the different studied cross sections of Nubia Lake. The CCHE2D is used to predict all sections for the year 2010 and the year 2020. In addition, available data of cross section in year 1964 is used to calculate the deposited area for all sections.

The four trails used cross sections' data of year 1964 to calculate the deposited area; see an example in section No. 19 as shown in Figs. 11 and 12. Depending on a procedure similar to that used in the traditional method, accumulated deposited volume (AcDV) in Sudanese part, total accumulated volume (TAV), and annual deposited volume (ADV) are calculated for the four trails (see Table 3). Finally, the life time span of dead zone (LTSDZ) and life time span of life zone (LTSLZ) are calculated and tabulated in Table 4.

8 Conclusions and Recommendations

The two-dimensional numerical model CCHE2D was used to study the sedimentation processes for Nubia Lake from km 500 to km 350 upstream Aswan High Dam with a total length of 150 km. The calibrated and verified CCHE2D model is capable of simulating the sedimentation process in Nubia Lake. It has been applied to predict the different cross sections of Nubia Lake for the year 2010 and the year 2020. The results were used to estimate the life time span. The life time span of

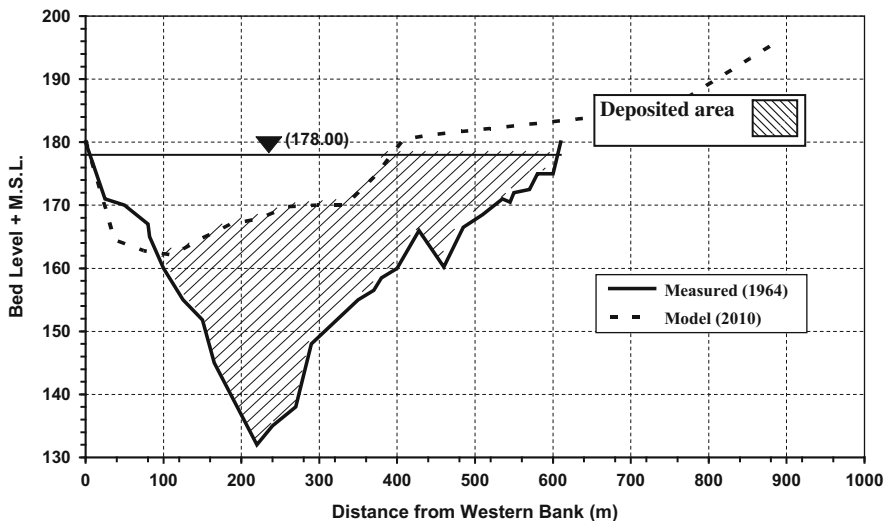


Fig. 11 Sediment accumulation at cross section 19 km 466 upstream AHD using the CCHE2D for the year 2010

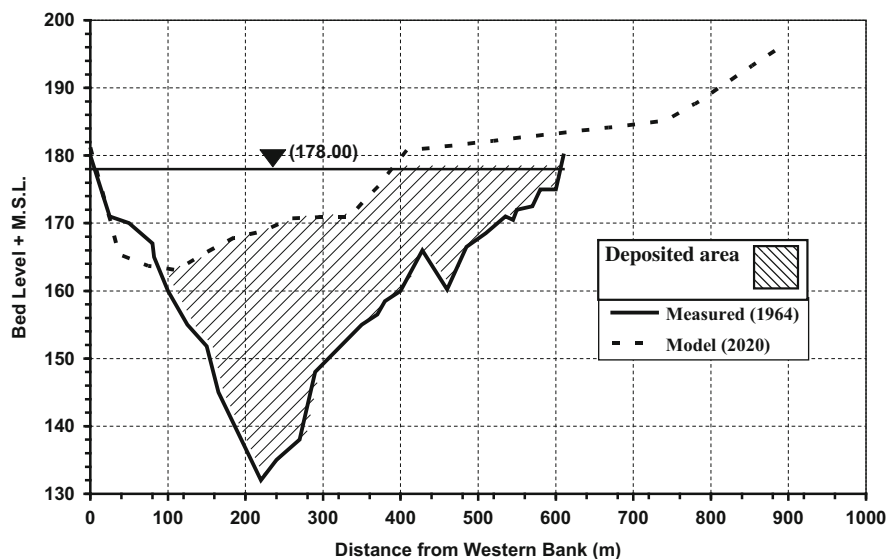


Fig. 12 Sediment accumulation at cross section 19 km 466 US AHD using the CCHE2D for the year 2020

dead zone, LTSDZ, is equal to 254 years, and the life time span of life zone, LTSLZ, is equal to 964 years. It should be noted that this life time span will not be significantly affected in the future due to the fact that after the construction of the GERD which will retain the sediment in its reservoir. However, the pattern of the accumulated sediment in the lake will be modified as a result of the almost clear coming inflow to AHDR. The authors highly recommend a hydrodynamic study to investigate the change in the sedimentation patterns due to different scenarios of the sediment concentration of incoming flow.

Acknowledgment The authors would like to thank the Water Technology Association (WTA) for the permission to republish some of the materials of the paper titled ““Predication of life time span of high Aswan dam reservoir using CCHE2D simulation model”” that was presented at the 14th International Water Technology Conference (IWTC14).

Table 4 Computed life time span via the computations of the deposited volumes in AHDR for the periods 1964–2007 (using the traditional method), 1964–2010, and 1964–2020 (using the CCHE2D)

Sec. code	Sec. length (km)	Dep. Vol. (Mm ³) Traditional 1964–2007	Dep. Vol. (Mm ³) CCHE2D 1964–2010	Dep. Vol. (Mm ³) CCHE2D 1964–2020
23	23.25	108.83	113.99	128.02
19	19.75	158.23	162.41	169.52
16	17.50	241.51	249.92	265.01
13	16.25	297.92	306.79	323.13
10	13.75	325.55	331.64	344.13
8	10.75	229.42	232.75	246.80
6	12.50	306.28	301.82	327.79
3	11.00	348.95	357.19	594.47
D	5.25	194.68	200.05	260.26
28	4.00	224.00	236.38	286.68
27	5.50	571.68	605.97	698.64
26	6.00	731.12	763.65	825.78
25	5.00	193.14	215.93	391.89
24	7.25	601.88	634.98	794.05
22	4.75	211.7	222.27	262.32
Sud. AcDV (Mm ³)		4,744.89	4,936.00	5,918.50
TAV (Mm ³)		5,693.90	5,922.89	7,102.18
ADV (years)		132.42	128.75	126.82
LTSDZ (years)		239	245	249
LTSLZ (years)		924	949	964

Appendix: Initial and Boundary Conditions Data of Section 4

See Tables 5–9.

Table 5 Typical surveyed coordinates of C.S. No. 23 (378.5 km US AHD) NRI [29]

x	Y	x	y	x	y	x	y	X	y
0	196.19	162.57	171.02	238.26	169.34	278.99	168.66	444.45	168.49
8	195.8	164.13	170.92	240.97	169.21	281.64	168.84	445.89	168.40
54.32	192.26	165.49	170.81	243.69	169.36	281.95	168.79	447.21	168.49
105	186.7	166.70	170.60	246.42	169.47	284.32	168.59	447.44	168.21
112.05	176.4	167.86	170.68	249.15	169.78	285.30	168.67	448.99	168.49
128.32	172.62	169.00	170.54	251.85	169.65	287.02	168.82	450.04	168.16
130.68	172.43	170.18	170.36	254.56	169.72	288.62	168.84	450.53	168.44
133.01	172.24	171.39	170.48	257.28	169.72	289.77	168.83	452.04	168.22
135.48	171.90	172.65	170.44	260.06	169.62	291.89	168.79	452.75	168.20
138.02	171.77	173.93	170.33	263.04	169.44	292.56	168.84	453.55	168.48
140.63	171.39	175.20	170.24	265.98	169.25	295.30	168.76	476.3	176.4
143.28	171.20	176.44	170.04	266.11	169.17	295.32	168.82	480.55	178.94
145.95	171.24	177.69	169.94	268.58	169.08	298.08	168.80	484.76	181.26
148.85	171.21	179.01	169.88	269.20	168.98	298.62	168.79	488.52	182.69
151.53	171.11	180.41	170.13	271.16	168.92	300.80	168.79	580.35	182.98
154.12	170.96	181.84	170.08	272.38	169.32	302.28	168.82	632.6	183.25
156.55	171.16	223.12	170.04	273.75	169.27	303.53	168.82	687.93	185.14
158.78	171.22	225.45	170.00	275.45	169.18	305.62	168.82	700.91	186.04
160.78	171.07	227.88	170.04	276.37	169.09	306.28	168.88	714.51	187.21

Table 6 Velocity and water level at the cross sections of the study area, NRI [29]

C.S. code	Name	Distance US AHD (km)	Date	Mean velocity (m/s)	Water level at section (m)
23	Daka	487.50	6/5/2003	0.41	175.55
19	Okma	466.00	7/5/2003	0.34	175.51
16	Malik EL Nasser	448.00	8/5/2003	0.25	175.24
13	EL Dowashate	431.00	9/5/2003	0.32	175.16
10	Atheri	415.50	10/5/2003	0.26	175.10
8	Semna	403.50	11/5/2003	0.20	175.08
6	Kajnarity	394.00	12/5/2003	0.18	175.03
3	Mourshed	378.50	13/5/2003	0.21	174.95
D	Gomi	372.00	14/5/2003	0.16	174.93
28	Madik Amka	368.00	15/5/2003	0.23	174.90
27	Amka	364.00	15/5/2003	0.18	174.90
26	Second cataract	357.00	16/5/2003	0.05	174.87
25	Abel kader	352.00	17/5/2003	0.05	174.84
24	Doghim	347.00	18/5/2003	0.08	174.82
22	Debrosa	337.50	19/5/2003	0.08	174.80

Table 7 Measured water level and discharge in AHDR, Amary [19]

Years		Discharge BCM	Water level (m)	Years		Average discharge BCM	Average water level (m)
1968	1969	80.96	151.1	1988	1989	110.85	164.41
1969	1970	82.38	153.83	1989	1990	75.8	163.77
1970	1971	91.91	159.68	1990	1991	70.04	162.5
1971	1972	90.43	162.49	1991	1992	81.86	163.98
1972	1973	64.47	158.2	1992	1993	88.07	167.45
1973	1974	89.73	161.71	1993	1994	91.19	169.64
1974	1975	95.26	165.6	1994	1995	94.59	172.34
1975	1976	115.71	172.42	1995	1996	81.38	172.76
1976	1977	80.47	171.7	1996	1997	95.55	175.5
1977	1978	90.55	172.52	1997	1998	73.53	174.75
1978	1979	85.28	173.04	1998	1999	120.62	175.79
1979	1980	70.5	171.27	1999	2000	107.47	175.85
1980	1981	79.51	171.13	2000	2001	94.75	175.7
1981	1982	81.76	170.36	2001	2002	95.58	175.14
1982	1983	64.88	165.87	2002	2003	71.1	172.06
1983	1984	73.19	163.6	2003	2004	80.13	171.8
1984	1985	56.38	156.37	2004	2005	72.73	169.59
1985	1986	78.69	157.23	2005	2006	76.88	168.65
1986	1987	66.86	154.65	2006	2007	105.42	173.42
1987	1988	63.08	151.7				

Table 8 Sieve analysis of bed samples, Makary [12]

Sec. (23)	Diameter (mm)	0.1	0.2	0.3	0.5
	Passing age%	2	8	40	50
Sec. (19)	Diameter (mm)	0.01	0.1	0.17	0.3
	Passing age%	3	19	48	30
Sec. (16)	Diameter (mm)	0.1	0.17	0.2	0.3
	Passing age%	10	40	30	20
Sec. (13)	Diameter (mm)	0.001	0.01	0.1	0.4
	Passing age%	3	6	21	70
Sec. (10)	Diameter (mm)	0.0001	0.001	0.01	0.1
	Passing age%	8	32	30	30
Sec. (8)	Diameter (mm)	0.0001	0.001	0.01	0.1
	Percentage %	3	15	22	60
Sec. (6)	Diameter (mm)	0.0001	0.001	0.01	0.1
	Passing age%	5	27	41	27
Sec. (3)	Diameter (mm)	0.0001	0.001	0.01	0.1
	Passing age%	5	35	42	18
Sec. (D)	Diameter (mm)	0.0001	0.001	0.01	0.1
	Passing age%	5	30	35	30
Sec. (28)	Diameter (mm)	0.0001	0.001	0.01	0.1

(continued)

Table 8 (continued)

	Passing age%	3	22	40	35
Sec. (27)	Diameter (mm)	0.0001	0.001	0.01	0.1
	Passing age%	5	35	40	20
Sec. (26)	Diameter (mm)	0.0001	0.001	0.01	0.1
	Passing age%	5	27	43	25
Sec. (25)	Diameter (mm)	0.0001	0.001	0.01	0.1
	Passing age%	7	38	40	15
Sec. (24)	Diameter (mm)	0.0001	0.001	0.01	0.1
	Passing age%	7	33	48	12
Sec. (22)	Diameter (mm)	0.0001	0.001	0.01	0.1
	Passing age%	10	55	23	12

Table 9 Sieve analysis of suspended samples, Makary [12]

Sec. (23)	Diameter (mm)	0.000001	0.00001	0.000001	0.00001
	Passing age%	5	55	5	55
Sec. (19)	Diameter (mm)	0.000001	0.00001	0.000001	0.00001
	Passing age%	0	30	0	30
Sec. (16)	Diameter (mm)	0.000001	0.00001	0.000001	0.00001
	Passing age%	5	45	5	45
Sec. (13)	Diameter (mm)	0.000001	0.00001	0.000001	0.00001
	Passing age%	22	48	22	48
Sec. (10)	Diameter (mm)	0.000002	0.00001	0.000002	0.00001
	Passing age%	8	47	8	47
Sec. (8)	Diameter (mm)	0.000001	0.00001	0.000001	0.00001
	Percentage %	0	15	0	15
Sec. (6)	Diameter (mm)	0.000001	0.00001	0.000001	0.00001
	Passing age%	42	28	42	28
Sec. (3)	Diameter (mm)	0.000001	0.00001	0.000001	0.00001
	Passing age%	30	30	30	30
Sec. (D)	Diameter (mm)	0.000001	0.00001	0.000001	0.00001
	Passing age%	30	30	30	30
Sec. (28)	Diameter (mm)	0.000001	0.00001	0.000001	0.00001
	Passing age%	30	30	30	30
Sec. (27)	Diameter (mm)	0.000001	0.00001	0.000001	0.00001
	Passing age%	30	30	30	30
Sec. (26)	Diameter (mm)	0.000001	0.00001	0.000001	0.00001
	Passing age%	30	30	30	30
Sec. (25)	Diameter (mm)	0.000001	0.00001	0.000001	0.00001
	Passing age%	30	30	30	30
Sec. (24)	Diameter (mm)	0.000001	0.00001	0.000001	0.00001
	Passing age%	30	30	30	30
Sec. (22)	Diameter (mm)	0.000001	0.00001	0.000001	0.00001
	Passing age%	30	30	30	30

References

1. World Commission on Dams (2000) Dams and development: a framework for decision making. Report. Earthscan, London
2. Morris G, Fan J (1998) Reservoir sedimentation handbook. McGraw-Hill, New York
3. Hargrove W, Johnson D, Snethen D, Middendorf J (2010) From dust bowl to mud bowl: sedimentation, conservation measures, and the future of reservoirs. *J Soil Water Conserv* 65 (1):14A–17A. doi:[10.2489/jswc.65.1.14A](https://doi.org/10.2489/jswc.65.1.14A)
4. Wang Z, Hu C (2009) Strategies for managing reservoir sedimentation. *Int J Sediment Res* 24 (4):369–384. doi:[10.1016/S1001-6279](https://doi.org/10.1016/S1001-6279)
5. Minear J, Kondolf G (2009) Estimating reservoir sedimentation rates at large spatial and temporal scales: a case study of California. *Water Resour Res* 45:W12502. doi:[10.1029/2007WR006703](https://doi.org/10.1029/2007WR006703)
6. Wang G (2005) Sedimentation problems and management strategies of Sanmenxia Reservoir, Yellow River, China. *Water Resour Res* 41:W09417. doi:[10.1029/2004WR003919](https://doi.org/10.1029/2004WR003919)
7. Soler-López LR (2001) Sedimentation survey results of the principal water-supply reservoirs of Puerto Rico, USGS Water Resources of the Caribbean. <http://vi.water.usgs.gov/public/reports/soler.html>
8. Angulo J, Jenkins A, Lebedev A, McNeff N (2015) Assessing the lifespans of reservoirs in region 2 of Puerto Rico. Annual report, 2015. Worcester Polytechnic Institute, Worcester
9. Issa E, Al-Ansari N, Sherwany G, Knutsson S (2013) Sedimentation processes and useful life of Mosul Dam Reservoir, Iraq. *Eng J* 5:779–784
10. Dalu T, Tambara E, Clegg B, Chari L, Nhwatiwa T (2013) Modeling sedimentation rates of Malilangwe reservoir in the south-eastern lowveld of Zimbabwe. *Appl Water Sci* 3:133–144. doi:[10.1007/s13201-012-0067-9](https://doi.org/10.1007/s13201-012-0067-9)
11. Wissler D, Frolking S, Hagen S, Bierkens M (2013) Beyond peak reservoir storage? A global estimate of declining water storage capacity in large reservoirs. *Water Resour Res* 49:5732–5739. doi:[10.1002/wrcr.20452](https://doi.org/10.1002/wrcr.20452)
12. Makary A (1982) Sedimentation in the High Aswan Dam Reservoir. Ph.D. thesis, Faculty of Engineering, Ain Shams University, Egypt
13. El-Moattassem M, Makary A (1988) Sedimentation balance in the Aswan High Dam Reservoir. Report 110 NRI. Cairo, Egypt
14. Shalash S (1980) Effect of sedimentation on storage capacity of high Aswan Dam Lake. Paper No. 56, El-Qanater, Egypt
15. Dahab A (1983) Lake Nasser area between Abu-Simble and Dall cataract. Ph.D. thesis, University of Ain Shams, Egypt
16. Abdel-Aziz TM (1991) Numerical modeling of sediment transport and consolidation in the Aswan High Dam Reservoir. M.Sc. thesis, Laboratory of hydrology, Free University of Brussels, VUB, Belgium
17. Abdel-Aziz TM (1997) Prediction of bed profile in the longitudinal and transverse direction in Aswan High Dam Reservoir. Ph.D. thesis, Cairo University, Giza, Egypt
18. El-Sersawy H (2005) Development of decision support system (D.S.S) for Aswan High Dam Reservoir sedimentation. National Water Research Center (N.W.R.C.), Cairo
19. Amary W (2008) Study the sedimentation inside High Aswan Dam Reservoir. M.Sc. thesis, Faculty of Engineering, Cairo University, Egypt
20. Moussa A (2012) Predicting the deposition in the Aswan High Dam Reservoir using a 2-D model. *Ain Shams Eng J* 4(2):143–153
21. Hekal N, Abdel-Aziz TM (2015) Effect of transverse water velocity distribution on sedimentation at Aswan High Dam Reservoir. In: Fifteenth international water technology conference, IWTC15. www.iwtc.info
22. Ziada W (2016) Sedimentation analysis for Aswan High Dam Reservoir. Ph.D. thesis, Benha University, Egypt

23. Hassan WE (2015) Impact of the upper River Nile projects on the lake of High Aswan Dam. Ph.D. thesis, Al-Azhar University, Cairo, Egypt
24. Elsayahbi M, Negm AM, Ali K (2016) Correlating the velocity profiles to the sediment profiles of the active sedimentation zone of Aswan High Dam Lake. In: Nineteenth international water technology conference, IWTC19, Sharm El Sheikh. <http://www.iwtc.info>
25. Elsaheed G, Aziz M, Ziada W (2016) Sedimentation analysis and prediction for Aswan High Dam Reservoir. *J Sci Eng Res* 3(4):302–312
26. Fathy I (2010) Evaluation of water resources projects in Egypt. M.Sc. thesis, Faculty of Engineering, Zagazig University, Egypt
27. Negm AM, Abdulaziz T, Nassar M, Fathy I (2010) Predication of life time span of High Aswan Dam Reservoir using CCHE2D simulation model. In: 14th International water technology conference, IWTC 14, Cairo, Egypt, pp 611–626
28. Zhang Y (2005) CCHE2D-GUI – graphical user interface for the CCHE2D model. User's manual – version 2.2. Technical Report No. NCCHE-TR-2005-03, The University of Mississippi
29. NRI (2003) Aswan High Dam Lake. Final report, Nile Research Institute, National Water Research Center, Ministry of Water Resources and Irrigation, El-Qanater, Egypt



<http://www.springer.com/978-3-319-59086-8>

The Nile River

Negm, A. (Ed.)

2017, XVII, 741 p., Hardcover

ISBN: 978-3-319-59086-8